Korean J. Chem. Eng., 37(2), 374-379 (2020)
DOI: 10.1007/s11814-019-0449-x

pISSN: 0256-1115
eISSN: 1975-7220

Si_3N_4 etch rates at various ion-incidence angles in high-density CF_4, CHF_3, and C_2F_6 plasmas

Jun-Hyun Kim* and Chang-Koo Kim,†**

*Institute of NT-IT Fusion Technology, Ajou University, 206 Worldcup-ro, Yeongtong-gu, Suwon 16499, Korea
**Department of Chemical Engineering and Department of Energy Systems Research, Ajou University,
206 Worldcup-ro, Yeongtong-gu, Suwon 16499, Korea

(*Received 22 September 2019 • accepted 1 December 2019*)

Abstract−The behavior of Si_3N_4 etching with ion-incidence angle in high-density CF_4, CHF_3, and C_2F_6 plasmas was investigated to understand the effect of discharge chemistry on the etch characteristics of Si_3N_4. The normalized etch yield (NEY) plots suggest that for all plasmas considered herein, physical sputtering is more prevalent than ion-assisted chemical etching as the Si_3N_4 etching mechanism. In the cases of the CF_4 and C_2F_6 plasmas, the NEYs at an ion-incidence angle of 60° were greater than unity because the thickness and the fluorine-to-carbon (F/C) ratio of the steady-state fluorocarbon films (st-st FC films) on the Si_3N_4 surfaces decreased and increased, respectively, as the ion-incidence angle was increased from 0° to 60°. In contrast, the NEY at this angle in the CHF_3 plasma was close to unity, as a result of a small change (or a very marginal decrease) in the thickness and the F/C ratio of the st-st FC film. Additionally, the NEY at an ion-incidence angle of 60° was higher in C_2F_6 plasma compared to CF_4 plasma because the changes in the thickness and the F/C ratio of the st-st FC film were greater in the C_2F_6 plasma than those in the CF_4 plasma.

Keywords: Si_3N_4 Etching, Ion-incidence Angle, Etching Mechanism, Steady-state Fluorocarbon Film

INTRODUCTION

In the fabrication of semiconductor devices, silicon nitride (Si_3N_4) is utilized as diffusion and ion-implantation masks, etch-stop layers, and gate spacers [1,2]. During the etching of Si_3N_4 films, both high and low etch selectivities with respect to other materials (e.g., SiO_2) are required depending on the application. For instance, plasma stripping of Si_3N_4 masks after local oxidation of silicon requires selective etching of Si_3N_4 over SiO_2 [3]. In contrast, high etch-selectivity of SiO_2 in regard to Si_3N_4 is required in self-aligned contact etching [4-6].

The Si_3N_4 etch rates are likely to change at corners and on inclined surfaces. Consequently, Si_3N_4 exhibits different etch selectivity on curved and flat surfaces. To realize control over the etch selectivity and etch profiles, it is crucial to understand the etch rate of Si_3N_4 at various surface angles.

To study the etch rate of the Si_3N_4 for various surface angles during plasma etching, the incidence of ions on the surface of the substrate should occur at arbitrary angles. As a sheath is always formed along the surface of the substrate in contact with the plasma, ions in the plasma arrive at the substrate vertically, regardless of the angle of the substrate, assuming that there are no ion-neutral collisions within the sheath. Hence, inclining the substrate in the plasma is ineffective for achieving control over the direction of ion-incidence on the surface of the substrate.

Methods, including use of ion beam etching [7] and V-groove microstructures [4,8], have been applied in the study of etch rate in Si_3N_4 at various angles. These methods can measure the etch rates on inclined surfaces, despite some critical limitations. As a result of lower operating pressure of the ion beam etching system, its radical concentration is significantly lower compared to a conventional plasma etching system. In regards to V-groove microstructures, there is a limited number of controllable ion-incidence angles.

Fluorocarbon gases such as CF_4 and CHF_3 were used to study the etch rate of Si_3N_4 at various angles under the different etching conditions in the cited work. Since the etch characteristics (e.g., etch rate) are affected by discharge chemistry, it is required to compare the behavior of Si_3N_4 etching with ion-incidence angle in various fluorocarbon plasmas under the identical etching conditions. A systematic comparison of the effect of discharge chemistry on the Si_3N_4 etch rates with ion-incidence angle has not been presented.

This work reports on the etch rate of Si_3N_4 at various ion-incidence angles in high-density CF_4, CHF_3, and C_2F_6 plasmas. A Faraday cage was used to investigate the etch rate of Si_3N_4 at various ion-incidence angles since it can be utilized to precisely control the ion-incidence angle under practical plasma etching conditions [9-14]. Furthermore, the effect of discharge gas on the etch rate of Si_3N_4 at various ion-incidence angles was investigated based on the variations in the Si_3N_4 etch rate and the characteristics of the steady-state fluorocarbon film formed on the substrate surface with ion-incidence angle.

EXPERIMENTAL

Fig. 1 shows the etching apparatus where a high-density plasma

†To whom correspondence should be addressed.
E-mail: changkoo@ajou.ac.kr
Copyright by The Korean Institute of Chemical Engineers.

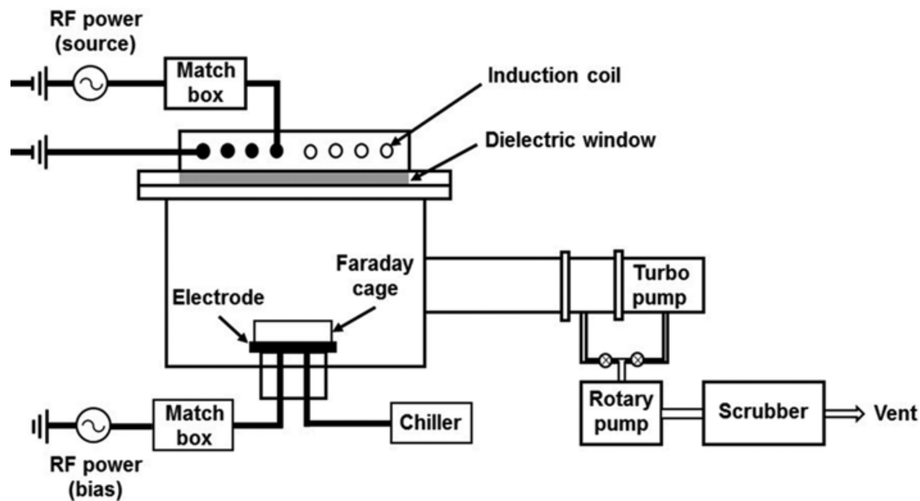

Fig. 1. Schematic of an inductively coupled plasma system.

was generated to carry out Si_3N_4 etching. A plasma was ignited through the application of radio-frequency (rf) source power (YoungSin, YSE-15MH) with a frequency of 13.56 MHz to an induction coil via a matching network. The source power's matching network consisted of a fixed capacitor (250 pF) and a variable capacitor (125-500 pF). The induction coil was water-cooled to avoid over-heating of the coil. To bias a substrate independently of source power, another rf bias power (YoungSin, YSE-06MF) was separately applied to the electrode via a matching network. The matching network for the bias power consisted of two variable capacitors (125-500 pF) and a coil. Consequently, the plasma was ignited in an inductively coupled manner.

The plasma was ignited in a cylindrical reaction chamber, then pumped using a 400 liter/s turbo molecular pump (Alcatel, ATC 400C). The turbo molecular pump was backed by a two-stage rotary mechanical pump (Edwards, E2M80). To allow visual inspection of the plasma, a 20 mm-diameter quartz window was placed on the sidewall of the reaction chamber.

The direction of ions incident on the substrate was controlled using a Faraday cage attached to the electrode (see Fig. 2). The Faraday cage was a closed cylindrical container consisting of a sidewall and a top grid. Both the cylindrical sidewall and the top grid were made of stainless steel. The grid diameter and pitch measured 25 and 229 μm, respectively.

If one considers a typical plasma condition (plasma density=1×10^{10} cm^{-3}, electron temperature=1 eV), the Debye length is 74 μm. Additionally, if a bias power is applied to the electrode, the sheath thickness will exceed several hundreds of mm. Since the sheath thickness is greater than the grid diameter (25 μm), the presence of the grid does not affect the plasma. The sheath then forms along the grid plane as though the grid opening were a solid wall. Thus, ions enter the Faraday cage perpendicular to the grid plane regardless of the slope of the substrate holder inside the cage. Consequently, the angle of ions incident on the substrate can be controlled by varying the angle of the substrate holder. The ion-incidence angle (θ) is defined as the angle between the direction of ion-incidence and the surface normal to the substrate, which is the same as the angle of the substrate holder.

The substrate consisted of a Si_3N_4 film (500 nm in thickness) on a Si wafer, as shown in Fig. 3. The Si_3N_4 films were grown through the low-pressure chemical vapor deposition technique. The substrate was cut into rectangular specimens (10×5 mm^2) and placed on the substrate holder.

CF_4, CHF_3, and C_2F_6 were separately utilized as discharge gases for Si_3N_4 Etching. The process conditions were identical for all discharge gases: source power=250 W, bias voltage=−1,200 V, cham-

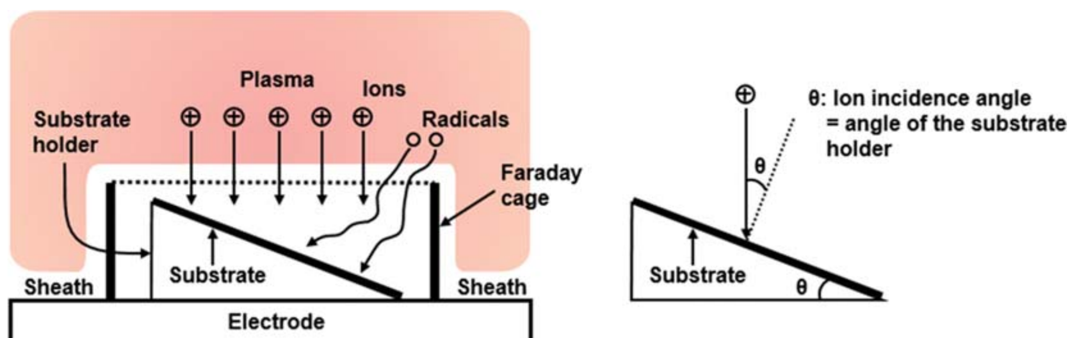

Fig. 2. Schematic of a Faraday cage.

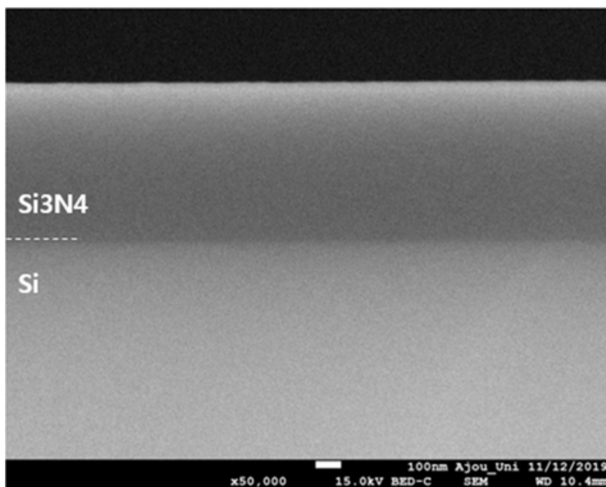

Fig. 3. Cross-sectional scanning electron microscopy image of the sample.

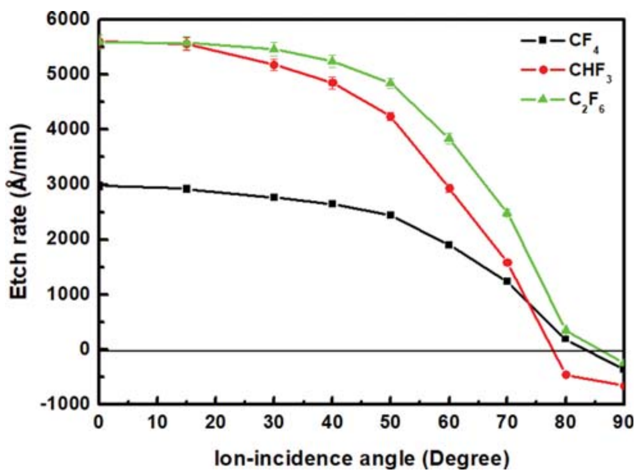

Fig. 4. Change in the etch rates of Si_3N_4 with ion-incidence angle in CF_4, CHF_3, and C_2F_6 plasmas.

ber pressure=10 mTorr, and gas flow rate=30 sccm.

A thickness meter (model SpectraThick 2000-Deluxe) was used to obtain the etch rates. The etch rates were measured three times for each condition and were averaged to obtain the final data. Deviations for all data were within 5%. The thickness and fluorine-to-carbon (F/C) ratio of the steady-state fluorocarbon film (st-st FC film) formed on the Si_3N_4 surface were obtained using an X-ray photoelectron spectroscope (XPS, Thermo Electron, K-Alpha). Calculation of the thickness and F/C ratio of the st-st FC film that formed on the surface of the substrate was based on the literature [15].

RESULTS

Fig. 4 illustrates the change in the etch rates of Si_3N_4 with ion-incidence angle in CF_4, CHF_3, and C_2F_6 plasmas. The etch rates decreased continuously with an increase in the ion-incidence angle in all the plasmas. At an ion-incidence angle of 90°, the etch rates were negative, indicating presence of film deposition rather than etching at this angle. In fluorocarbon plasmas, substrate etching and fluorocarbon film deposition occur simultaneously since fluorocarbon films (C_xF_y) are subject to forming on the surface of the object in contact with these plasmas. The fluorocarbon films grow in any direction; therefore, the net deposition of the fluorocarbon films on the vertical surface (90° from the surface normal) of the substrate is observed frequently. At ion-incidence angles of up to 70°, the etch rates of Si_3N_4 in the CHF_3 and C_2F_6 plasmas were higher compared to those in CF_4 plasma. In the CHF_3 plasma, the etch rates of Si_3N_4 decreased rapidly compared to those in the CF_4 and C_2F_6 plasmas, indicating that film deposition was initially observed at an ion-incidence angle of 80°. This phenomenon is visualized more clearly through the normalized etch rate (NER).

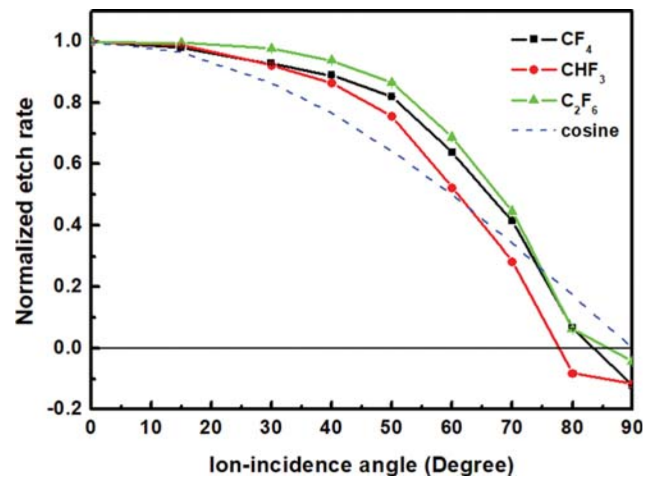

Fig. 5. Change in the NERs of Si_3N_4 with ion-incidence angle in CF_4, CHF_3, and C_2F_6 plasmas.

Fig. 5 shows the change in the NERs of Si_3N_4 with ion-incidence angle in CF_4, CHF_3, and C_2F_6 plasmas. The NER is defined as the etch rate at a specific angle normalized in regard to the etch rate of the horizontal surface, which is equal to etch rate (θ)/etch rate (0°). Regarding the NER curve, the dotted line represents a cosine curve corresponding to the changes in the flux of ions with respect to their incident angle. In all the plasmas, the value of NERs exceeded that of cosine at ion-incidence angles of up to 60°. As a result of the rapid decrease in the etch rate with increasing ion-incidence angle in the CHF_3 plasma, at the ion-incidence angle of 70°, the NER in the CHF_3 plasma was lower than the cosine value, while those in the CF_4 and C_2F_6 plasmas were higher compared to the cosine value.

The changes in the etch rate and the NER with ion-incidence angle are dependent on the ion flux variation. Since the etch yield, which is equivalent to the etch rate per ion flux on the substrate, excludes the effect of ion flux variation with ion-incidence angle, it is more suitable to use the etch yield rather than the etch rate for the study of ion-surface interactions for various ion-incidence angles [16].

Fig. 6 illustrates the change in the normalized etch yields (NEYs) of Si_3N_4 with ion-incidence angle in CF_4, CHF_3, and C_2F_6 plasmas. Similar to the definition of the NER, the NEY is defined as etch

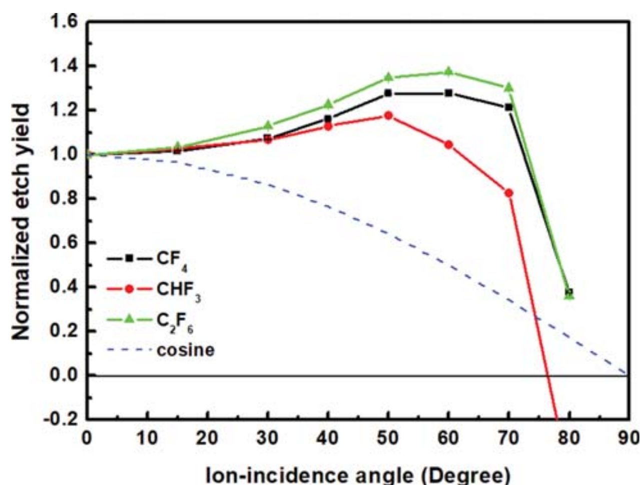

Fig. 6. Change in the NEYs of Si_3N_4 with ion-incidence angle in CF_4, CHF_3, and C_2F_6 plasmas.

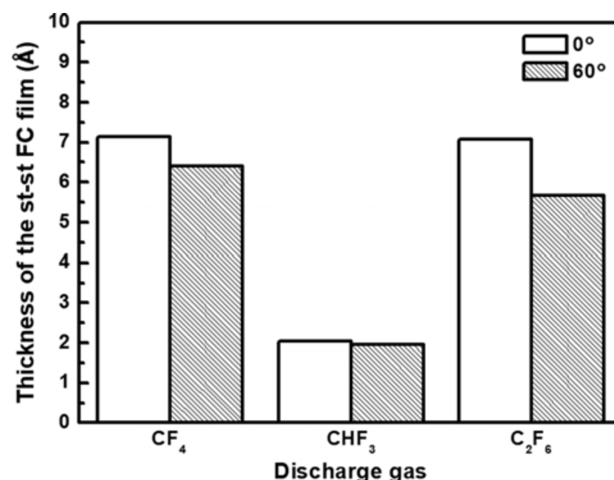

Fig. 7. Thickness of the st-st FC films formed on the surface of Si_3N_4 at ion-incidence angles of 0° and 60°, respectively, in CF_4, CHF_3, and C_2F_6 plasmas.

yield (θ)/etch yield (0°) which is given by the NER divided by cosθ. In all the plasmas, the NEYs of Si_3N_4 increased to a maximum and then decreased with an increase in the ion-incidence angle. However, the maximum NEY value and the ion-incidence angle at which it was observed are dependent on the discharge gas. In the CF_4 and C_2F_6 plasmas, the NEYs peaked at the ion-incidence angle of 60° with maximum values of 1.28 and 1.38, respectively. In the CHF_3 plasma, the maximum NEY value was 1.18 and occurred at the ion-incidence angle of 50°.

DISCUSSION

Since variations in the etch yield with the ion-incidence angle provide the etching mechanism information, the changes in the NEYs with ion-incidence angle as shown in Fig. 6 suggest that the etching mechanism of Si_3N_4 is dependent on the discharge gas. When the etch yield attains a maximum value between 40° and 70°, physical sputtering rather than ion-assisted chemical etching is known to play a major role during etching [17]. Hence, the etch yield plots of CF_4, CHF_3, and C_2F_6 plasmas as shown in Fig. 6 suggest that the relative significance of physical sputtering and ion-assisted chemical etching is influenced by the discharge gas used in Si_3N_4 etching.

The relative contribution of physical sputtering in the plasmas is notable. CHF_3 plasma showed the least maximum NEY value (1.18). Similarly, the maximum NEY value for CHF_3 plasma was obtained at the ion-incidence angle of 50° as opposed to 60° in the CF_4 and C_2F_6 plasmas. This suggests that the contribution of physical sputtering to the overall etching process in the CHF_3 plasma was less compared to that in CF_4 and C_2F_6 plasmas, despite the NEY curves showing that physical sputtering was the main etching mechanism in all the plasmas under the process conditions used in this study. This might be attributed to the presence of H in CHF_3 plasma. The formation of volatile etching products, including HCN, has been reported to be highly probable during Si_3N_4 etching in H-containing plasmas [5,18]. As CHF_3 contains H atoms, the CHF_3 plasma ought to produce a greater number of chemical reaction pathways than the CF_4 and C_2F_6 plasmas. Consequently, the contribution of physical sputtering to the overall etching in the CHF_3 plasma was reduced compared to the CF_4 and C_2F_6 plasmas. This can guide the selection of discharge chemistry for specific application during Si_3N_4 etching. When anisotropic etching is more important than selectivity control, CF_4 and C_2F_6 plasmas are appropriate. On the other hand, when the etch selectivity is more important than the anisotropic profile, a CHF_3 plasma is relevant because the contribution of physical sputtering to the overall etching is reduced in this plasma.

In addition, the etch yield curve can depend on the st-st FC film which is formed on the substrate of the fluorocarbon plasmas. The st-st FC film, which is formed due to the competition between production and consumption of fluorocarbons, suppresses the migration of ions and radicals within it [15,19]. Consequently, the features of the st-st FC films formed in the CF_4, CHF_3, and C_2F_6 plasmas were examined.

Fig. 7 displays the thickness of the st-st FC films formed on the Si_3N_4 surface at ion-incidence angles of 0° and 60°, respectively, in CF_4, CHF_3, and C_2F_6 plasmas. In the CF_4 and C_2F_6 plasmas, the thickness of the st-st FC films reduced as the ion-incidence angle was increased from 0° to 60°. In addition, the degree at which the film thickness decreased was higher in the C_2F_6 plasma (7.1 to 5.7 Å) compared to the CF_4 plasma (7.1 to 6.4 Å). In contrast, little change in the thicknesses of the st-st FC films of CHF_3 plasma was observed as the ion-incidence angle was increased from 0° to 60°. The change in the film thickness corresponds to the relative magnitude of the NEY in the CF_4, CHF_3, and C_2F_6 plasmas. As highlighted earlier, the st-st FC film inhibits ions and radicals from travelling within it. Since the st-st FC film served as an etch barrier, the etch yield was inversely proportional to the film thickness. Therefore, at an ion-incidence angle of 60°, the NEYs were higher than unity in the CF_4 (1.27) and C_2F_6 (1.37) plasmas, while being approximately unity in the CHF_3 (1.05) plasma. Similarly, at the ion-incidence angle of 60°, the NEY was higher in the C_2F_6 plasma compared to the CF_4 plasma owing to the notable change in thick-

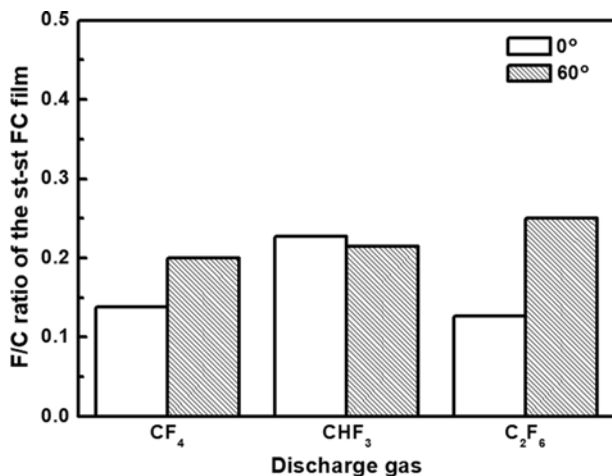

Fig. 8. F/C ratio of the st-st FC films formed on the surface of Si_3N_4 at ion-incidence angles of 0° and 60°, respectively, in CF_4, CHF_3, and C_2F_6 plasmas.

ness of the film in the C_2F_6 plasma (1.4 Å) than that in the CF_4 plasma (0.7 Å). The NEY value at this angle decreased in the order of C_2F_6>CF_4>CHF_3.

The relative magnitude of the NEY in the CF_4, CHF_3, and C_2F_6 plasmas was supported through the F/C ratio of the st-st FC film. Fig. 8 presents the F/C ratio of the st-st FC films formed on the surface of Si_3N_4 at ion-incidence angles of 0° and 60°, respectively, in the CF_4, CHF_3, and C_2F_6 plasmas. In regards to the CF_4 and C_2F_6 plasmas, the F/C ratios of the st-st FC films increased as the ion-incidence angle was increased from 0° to 60°. The change in the F/C ratio was more in the C_2F_6 plasma (from 0.13 to 0.25) than that in the CF_4 plasma (from 0.14 to 0.20). In contrast, the F/C ratios of the st-st FC films at ion-incidence angles of between 0° and 60° did not have an effect on the CHF_3 plasma. It is known that a fluorocarbon film with a lower F/C ratio is more strongly crosslinked, which increases the etch resistance [9]. Specifically, when the F/C ratio of the st-st FC film increases, the substrate on which the film is formed is etched to a greater degree. Therefore, based on the F/C ratios of the st-st FC films, it was confirmed that the NEYs at the ion-incidence angle of 60° were higher than unity in the CF_4 and C_2F_6 plasmas and approximately unity in the CHF_3 plasma. The results of the F/C ratio of the st-st FC films also supported that the NEY at the ion-incidence angle of 60° was higher in the C_2F_6 plasma than that in the CF_4 plasma.

CONCLUSIONS

An investigation on the Si_3N_4 etch rates at various ion-incidence angles was conducted in high-density CF_4, CHF_3, and C_2F_6 plasmas to understand the effect of discharge chemistry on Si_3N_4 etching. The etch rates of Si_3N_4 decreased continuously with an increase in the ion-incidence angle in all the plasmas. The etch rates decreased with increasing ion-incidence angle and were eventually negative at the ion-incidence angle of 90°, indicating the occurrence of film deposition instead of etching on the vertical surface.

The etch yield curves of the CF_4, CHF_3, and C_2F_6 plasmas implied that the prevalence of physical sputtering or ion-assisted chemical etching as the main mechanism of Si_3N_4 etching was governed by the discharge gas used in the process. The NEY of Si_3N_4 at various ion-incidence angles exhibited that the etching mechanism was more affected by physical sputtering compared to ion-assisted chemical etching in all the plasmas. However, the contribution of physical sputtering to the overall etching in the CHF_3 plasma was reduced relative to the ones in the CF_4 and C_2F_6 plasmas. This was because the H atoms in CHF_3 promoted the formation of volatile etch products such as HCN, which increased the number of chemical pathways available in the CHF_3 plasma compared to those in the CF_4 and C_2F_6 plasmas.

In addition, the dependence of the etch yield on the ion-incidence angle was investigated based on the features of the st-st FC film formed on the substrate. The thickness and the F/C ratio of the st-st FC films formed on the Si_3N_4 surface decreased and increased, respectively, as the ion-incidence angle was increased from 0 to 60° in the CF_4 and C_2F_6 plasmas. In contrast, the thickness and the F/C ratio of the st-st FC film showed no change or a marginal decrease at ion-incidence angles of between 0° and 60° in the CHF_3 plasma. Additionally, the extent of changes in the thickness and the F/C ratio of the st-st FC film was greater in the C_2F_6 plasma than in the CF_4 plasma. This corresponded to the relative magnitude of the NEY in the CF_4, CHF_3, and C_2F_6 plasmas; specifically, the NEY value at the ion-incidence angle of 60° decreased in the order of C_2F_6>CF_4>CHF_3. In addition, the NEYs at this angle were greater than unity in the CF_4 and C_2F_6 plasmas and approximately unity in the CHF_3 plasma.

During Si_3N_4 etching in various fluorocarbon plasmas such as CF_4, CHF_3, and C_2F_6 plasmas, the relative contribution of physical sputtering to the overall etching was dependent on discharge chemistry. Consequently, this work can provide information on the selection of discharge chemistry for specific application during Si_3N_4 etching.

ACKNOWLEDGEMENTS

This work was supported by the Korea Institute of Energy Technology Evaluation and Planning (KETEP) grant funded by the Korea Government Ministry of Trade, Industry and Energy (Grant No. 20172010104830), the National Research Foundation of Korea (NRF) grant funded by the Korea government (MEST) (Grant No. 2018R1A2B6002410), and the GRRC program of Gyeonggi province (GRRC AJOU 2016B03, Photonics-Medical Convergence Technology Research Center).

REFERENCES

1. Y. X. Li, P. J. French and R. F. Wolffenbuttel, *J. Vac. Sci. Technol. B*, **13**, 2008 (1995).
2. J. H. Choi, S. J. Kim, H. T. Kim and S. M. Cho, *Korean J. Chem. Eng.*, **35**, 1348 (2018).
3. B. E. E. Kastenmeier, P. J. Matsuo and G. S. Oehrlein, *J. Vac. Sci. Technol. A*, **17**, 3179 (1999).
4. M. Schaepkens, G. S. Oehrlein, C. Hedlund, L. B. Jonsson and H.-O. Blom, *J. Vac. Sci. Technol. A*, **16**, 3281 (1998).

5. M. Ito, K. Kamiya, M. Hori and T. Goto, *J. Appl. Phys.*, **91**, 3452 (2002).
6. M. Schaepkens, T. E. F. M. Standaert, N. R. Rueger, P. G. M. Sebel, G. S. Oehrlein and J. M. Cook, *J. Vac. Sci. Technol. A*, **17**, 26 (1999).
7. A. M. Barklund and H.-O. Blom, *J. Vac. Sci. Technol. A*, **10**, 1212 (1992).
8. A. M. Barklund and H.-O. Blom, *J. Vac. Sci. Technol. A*, **11**, 1226 (1993).
9. S.-W. Cho, C.-K. Kim, J.-K. Lee, S. H. Moon and H. Chae, *J. Vac. Sci. Technol. A*, **30**, 051301 (2012).
10. S.-W. Cho, J.-H. Kim, D. W. Kang, K. Lee and C.-K. Kim, *ECS J. Solid State Sci. Technol.*, **3**, Q215 (2014).
11. S.-W. Cho, J.-H. Kim, J. G. Bak and C.-K. Kim, *ECS Solid State Lett.*, **4**, 85 (2015).
12. J.-H. Kim, S.-W. Cho, C. J. Park, H. Chae and C.-K. Kim, *Thin Solid Films*, **637**, 43 (2017).
13. J.-H. Kim, S.-W. Cho and C.-K. Kim, *Chem. Eng. Technol.*, **40**, 2251 (2017).
14. J.-H. Kim, J.-S. Park and C.-K. Kim, *Thin Solid Films*, **669**, 262 (2019).
15. T. E. F. M. Standaert, C. Hudlund, E. A. Joseph and G. S. Oehrlein, *J. Vac. Sci. Technol. A*, **22**, 53 (2004).
16. B.-O. Cho, S.-W. Hwang, G.-R. Lee and S. H. Moon, *J. Vac. Sci. Technol. A*, **18**, 2791 (2000).
17. D. P. Hamblen and A. Cha-Lin, *J. Electrochem. Soc.*, **135**, 1816 (1988).
18. N. R. Rueger, J. J. Beulens, M. Schaepkens, M. F. Doemling, J. M. Mizra, T. E. F. Standaert and G. S. Oehrlein, *J. Vac. Sci. Technol. A*, **15**, 1881 (1997).
19. M. Schaepkens, T. E. F. M. Standaert, N. R. Rueger, P. G. M. Sebel, G. S. Oehrlein and J. M. Cook, *J. Vac. Sci. Technol. A*, **17**, 26 (1999).